Environmental Science & Technology

Article

Cite This: Environ. Sci. Technol. 2019, 53, 9289−9297

pubs.acs.org/est

Space, Time, and Size Dependencies of Greenhouse Gas Payback Times of Wind Turbines in Northwestern Europe

Louise C. Dammeier,*[,†] Jessica M. Loriaux,[†] Zoran J. N. Steinmann,[†] Daan A. Smits,[†] Ine L. Wijnant,[‡] Bart van den Hurk,[‡,¶] and Mark A. J. Huijbregts[†]

[†]Department of Environmental Science, Faculty of Sciences, Radboud University Nijmegen, Heyendaalseweg 135, 6525 AJ Nijmegen, The Netherlands

[‡]Royal Netherlands Meteorological Institute, Postbus 201, 3730 AE De Bilt, The Netherlands

[¶]Deltares, P.O. Box 177, 2600 MH Delft, The Netherlands

ABSTRACT: The net greenhouse gas benefits of wind turbines compared to their fossil energy counterparts depend on location-specific wind climatology and the turbines' technological characteristics. Assessing the environmental impact of individual wind parks requires a universal but location-dependent method. Here, the greenhouse gas payback time for 4161 wind turbine locations in northwestern Europe was determined as a function of (i) turbine size and (ii) spatial and temporal variability in wind speed. A high-resolution wind atlas (hourly wind speed data between 1979 and 2013 on a 2.5 by 2.5 km grid) was combined with a regression model predicting the wind turbines' life cycle greenhouse gas emissions from turbine size. The greenhouse gas payback time of wind turbines in northwestern Europe varied between 1.8 and 22.5 months, averaging 5.3 months. The spatiotemporal variability in wind climatology has a particularly large influence on the payback time, while the variability in turbine size is of lesser importance. Applying lower-resolution wind speed data (daily on a 30 by 30 km grid) approximated the high-resolution results. These findings imply that forecasting location-specific greenhouse gas payback times of wind turbines globally is well within reach with the availability of a high-resolution wind climatology in combination with technological information.

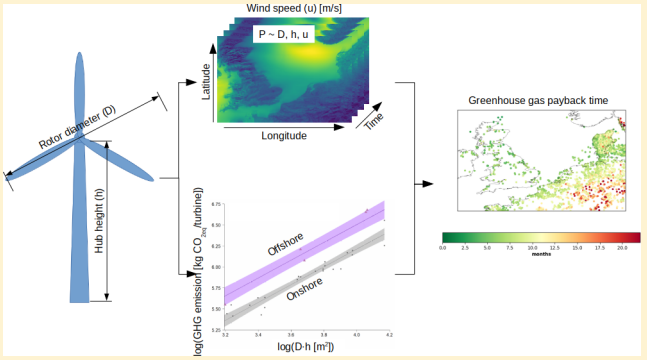

INTRODUCTION

Wind energy is becoming increasingly important in the world's electricity supply as it becomes cost competitive and the demand for sustainable energy is rising.[1] By the end of 2017, the cumulative capacity of all wind turbines installed globally reached over 539 GW, meeting approximately 5% of the world's electricity demand.[2] It is projected that wind could contribute 18% to 36% of the world's electricity production in 2050.[3,4]

The environmental performance of wind electricity is typically determined by means of a life cycle assessment (LCA),[5] which is a systematic approach to determine the environmental impact of a technology considering all the resources required and related emissions during the different stages of its life cycle.[6] For wind, the environmental impact per unit of electricity produced depends on the amount and type of materials used to build and maintain the wind turbine as well as the electricity produced over its life cycle.[7] Because it is virtually impossible to perform specific LCAs for all individual wind turbines worldwide, Caduff et al.[8] developed a regression model estimating the life cycle greenhouse gas (GHG) emission of onshore wind turbines as a function of rotor diameter and hub height. They found that the bigger the wind turbine, the lower the GHG emissions per unit of electricity produced. However, their analysis was focused on onshore turbines and did not take climatological variations of wind speed into account.

LCAs of wind turbines are typically based on the mean wind speed at hub height.[7−14] More recently, a comprehensive LCA study for wind electricity in Denmark built a model to estimate a wind turbine's life cycle GHG emissions based on technological scaling relationships and spatiotemporal information on wind speed data with approximately a 50 by 50 km grid resolution.[15,16] Their study emphasized the importance of including spatiotemporal variation of wind speed in the power calculations. The required spatiotemporal resolution of wind speed data to obtain reliable LCA results was, however, not analyzed in their study. To our knowledge, a comparison of the site-specific environmental performance of wind electricity on larger spatial scales that takes into account detailed spatiotemporal variability in the local wind resource is

Received: February 18, 2019
Revised: May 6, 2019
Accepted: July 3, 2019
Published: July 3, 2019

DOI: 10.1021/acs.est.9b01030
Environ. Sci. Technol. 2019, 53, 9289−9297

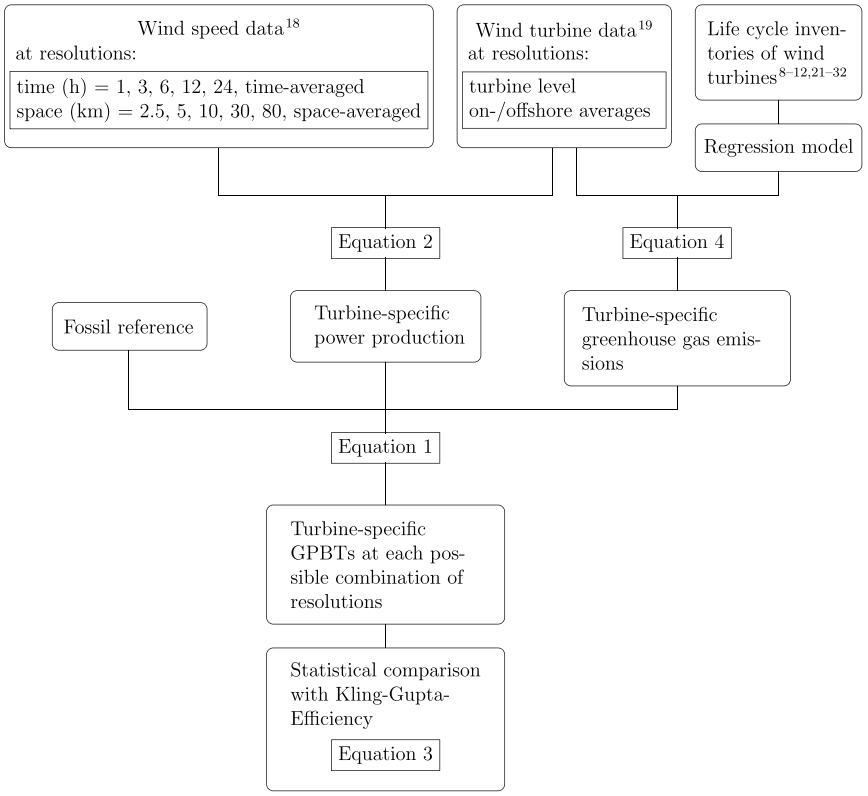

Figure 1. Schematic representation of the calculation of the turbine-specific greenhouse gas payback time (GPBT).

currently lacking. Moreover, it is not known which spatiotemporal resolution actually is sufficient to capture the variability in the wind resource in such an assessment.

Here, the greenhouse gas payback time (GPBT) of 4161 wind turbine locations in northwestern Europe was quantified, accounting for variability in both wind climatology and turbine technology. The GPBT is a commonly used metric to identify the environmental performance of wind energy compared with a fossil energy benchmark, which equals the time it takes until the total GHG savings due to the replacement of fossil energy by wind energy equals the GHG emissions during a turbine's life cycle.[17]

To simulate the yearly average power output of the individual wind turbines high-resolution wind data for 35 years on a 2.5 by 2.5 km grid[18] was combined with technical information for individual wind turbines.[19] The life cycle GHG emissions for onshore and offshore wind turbines were derived from the turbine size with an updated regression model based on the work by Caduff et al.[8] The importance of using a high-resolution wind climatology data set and turbine-specific data was assessed by analyzing the sensitivity of wind turbine GPBTs to (i) differences in spatiotemporal detail of wind speed and (ii) including or excluding differences in turbine size.

MATERIALS AND METHODS

Overview. The influence of time and space dependencies in wind speed and size variations of wind turbine characteristics on the environmental impacts was analyzed according to the steps shown in Figure 1. These steps are further explained below.

Greenhouse Gas Payback Time. The GPBT depends on the total emissions during the lifetime of the wind turbine and its power output, as well as the greenhouse gas emissions of the fossil energy reference. The GPBT (in months) of a wind turbine is calculated as

$$\mathrm{GPBT}_{\mathrm{turbine}} = \frac{\mathrm{GHG}_{\mathrm{turbine}}}{P_{\mathrm{turbine}} \cdot \mathrm{GHG}_{\mathrm{fossil}}} \quad (1)$$

where $\mathrm{GHG}_{\mathrm{turbine}}$ is the cumulative GHG emission resulting from the production and installation of the wind turbine (kg CO_2-eq/turbine), P_{turbine} the lifetime average electricity production of the wind turbine (kWh/month), and $\mathrm{GHG}_{\mathrm{fossil}}$ the GHG emission of the fossil energy benchmark (kg CO_2-eq/kWh). The average emission of natural gas-fired power plants of 0.5 kg CO_2-eq/kWh was chosen as reference for the whole study area.[20]

GHG Emissions of Wind Turbine Production. To calculate the GHG emissions, a regression model was developed that expresses GHG emissions of a turbine during its lifetime ($\mathrm{GHG}_{\mathrm{turbine}}$) as a function of rotor diameter (D) and hub height (h). For this, the model from Caduff et al.[8] was modified by expanding the underlying empirical data set[9−12,21−32] and including systematic differences in GHG emissions between onshore and offshore turbine production.[33] A Gaussian generalized linear model was applied using RStudio (RStudio Team, 2015), based on 28 wind turbine LCA studies of 22 on- and 6 offshore locations. Cross-validation was performed using a leave-one-out method.[34] The best model was chosen based on the Akaike information criterion (AIC).

Power Output. The turbine's power output $P_{\mathrm{turbine},i}$ at time i depends on the time-varying wind speed at hub height u_i (m/s) and the rotor diameter through

$$P_{\mathrm{turbine},i} = 0.5 \cdot \mu \cdot \mu_{\mathrm{Betz}} \cdot \rho \cdot A_{\mathrm{turbine}} \cdot u_i^{\,3} \quad (2)$$

DOI: 10.1021/acs.est.9b01030
Environ. Sci. Technol. 2019, 53, 9289−9297

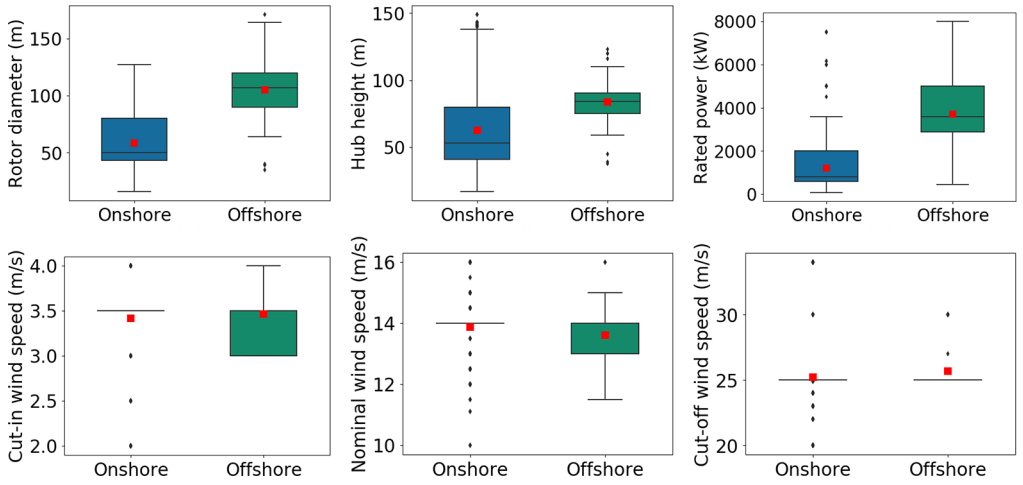

Figure 2. Box plots show the distribution of important technological wind turbine characteristics for the turbines in the data set. Blue bars are onshore turbines (n = 4061), and green bars are offshore turbines (n = 80). The plots show the three quartile values of the distribution, the 1.5 interquartile range represented by the whiskers, and the data points outside this range as individual values. The red dots represent the mean used for average turbine sizes.

where μ = 0.85 is the overall efficiency (including grid losses and machine downtime, among others),[35] μ_{Betz} the theoretical maximum power that a wind turbine can produce ($\frac{16}{27}$, Betz's law),[36] ρ the air density (1.225 kg/m^2), and $A_{turbine}$ the swept area (m^2) given by $0.25{\cdot}\pi{\cdot}D^2$. A wind turbine operates in a limited wind speed range (between cut-in and cut-out wind speeds), below and above which no electricity is produced. Above the rated wind speed the turbine is programmed to operate at its rated power output until it reaches the cut-out wind speed.

Data. *Wind Turbines.* Wind turbines in Northwestern Europe within the domain of 48°N to 60°N and −8°E to +12°E were included in this study. Their location and technical specifications were taken from The WindPower database,[19] which provides information on the turbines' hub heights and rotor diameters. This information is used in the calculation of the turbines' life cycle GHG emissions (eq 4) as well as their power output (eq 2). Data was available for 4161 wind power locations within the selected domain, of which 80 are offshore and 4081 are onshore. The included technological turbine characteristics are given in Figure 2.

Wind Speed. Wind speed data was derived from the KNMI North Sea Wind Atlas (KNW-Atlas).[18] This data set contains hourly wind speed data on a 2.5 by 2.5 km grid for all years between 1979 and 2013. The KNW-Atlas is based on ERA-Interim reanalysis data[37] downscaled with the high-resolution, nonhydrostatic weather forecasting model HARMONIE CY37h1.1.[38,39] It contains wind speeds at heights of 10, 20, 40, 60, 80, 100, 150, and 200 m. The KNW-Atlas has been validated[40,41] and produces accurate wind climatology up to 200 m above sea level. For the wind turbine locations, wind speed data at the nearest KNW-grid point were used. The wind speed at hub height was calculated by a linear interpolation of KNW-levels to the hub height. This wind speed was then used to calculate the average yearly power output for each wind turbine location over the full period of 35 years.

Statistical Analysis. *Technology versus Climatology.* In the reference situation, the turbines' GPBTs were calculated using the high-resolution data from the KNW-Atlas (2.5 by 2.5 km grid, hourly data). To assess the importance of knowing the location-specific turbine size and wind climatology, this reference was compared to the turbines' GPBTs for four scenarios in which variability characteristics were modified:

1. The importance of spatial variability in the GPBT calculations was assessed by using a **spatial average** of the wind data.
2. The importance of temporal variability was assessed by using a **temporal average** of the wind data.
3. The importance of spatial and temporal variability was assessed using a **spatial and temporal average** of the wind data.
4. The importance of technological variation was assessed using **average turbine sizes** for on- and offshore turbines.

Spatial average means that for every hour in the 35-year study period, the wind data of each grid point were averaged and used as wind speed value at that hour for every grid point in the domain prior to calculating the power output for that hour. Similarly, a temporal average means that all hourly wind speed values at a certain grid point were averaged and used for every time slot at that location. Using both the spatial and the temporal average, only one wind speed value was used for all turbines for the whole study period, resulting in only the technological variability of the wind turbines (e.g., hub height, diameter, and cut-in and cut-out wind speeds) remaining. Lastly, technological averages were created by using average onshore and offshore turbine characteristics based on the turbines in the study area, which are shown in Figure 2.

The Kling−Gupta efficiency (KGE) was used to calculate the effect of neglecting spatial, temporal, or technological variability. The KGE is a combination of correlation, bias, and variability between scenario n (constant wind in space, time, or both or constant turbine type) and the reference scenario and is defined as[42]

$$\mathrm{KGE}_n = 1 - \sqrt{(\beta_n - 1)^2 + (\gamma_n - 1)^2 + (r_n - 1)^2} \qquad (3)$$

with r_n the Pearson correlation coefficient between the GPBT, γ_n the variability ratio $((\sigma_n/\mu_n){\cdot}(\mu_r/\sigma_r))$, and β_n the bias ratio (μ_n/μ_r), with σ the standard deviation and μ the mean of the GPBT results, of scenario n (see above) compared to the reference scenario with a 2.5 by 2.5 km grid, hourly wind speed

DOI: 10.1021/acs.est.9b01030
Environ. Sci. Technol. 2019, 53, 9289−9297

data, and turbine-specific data. The KGE ranges from −∞ to 1 (1 being a perfect fit).

Importance of Spatial and Temporal Resolution. The importance of using a high spatial and temporal resolution in the GPBT calculations was investigated as well, because wind data on large spatial scales are usually available at coarser resolutions than used in this study.[43,44] For this, 25 data sets were created from the KNW-Atlas data by aggregating temporal and spatial resolutions to a coarser scale, based on typical resolutions of regional and global climate archives:[45]

- temporal resolution: 1 h (default), 3 h, 6 h, 12 h, and 24 h
- spatial resolution: 2.5 by 2.5 km (default), 5 by 5 km, 10 by 10 km, 30 by 30 km, and 80 by 80 km

Reduction of temporal and spatial resolutions was obtained by subsampling the default data at indicated space and time intervals. Daily wind speed data were constructed by sampling data at noon (12:00 UTC). GPBTs of the 4161 wind power locations were recalculated for the 25 additional data sets, and the results of each data set were evaluated against the reference data set using the KGE (see eq 3). All spatiotemporal analyses were carried out using NCL.[46]

RESULTS

Regression Model. The optimal AIC model fit to describe turbine life cycle GHG emission as a function of its diameter (D), hub height (h), and onshore/offshore technology indicator (T) was

$$\log(\mathrm{GHG}_{\mathrm{turbine}}) = c_0 + c_1 \cdot \log(D) + c_2 \cdot \log(h) + c_3 \cdot T \quad (4)$$

where $c_0 = 2.00[\pm 0.45]$ is the intercept, $c_1 = 1.27[\pm 0.50]$, $c_2 = 0.84[\pm 0.56]$, and $c_3 = 0.29[\pm 0.10]$. Figure 3 shows the regression lines for offshore and onshore wind turbines based on 28 LCA studies found in the literature.[8−12,21−32]

Reference Situation. Using the turbine-specific GHG emissions and wind data from the KNW-Atlas at the highest spatiotemporal resolution, GPBTs show a pronounced spatial pattern (Figure 4). The lowest values are located offshore and close to the coast (1.8 months as lowest GPBT), where wind speeds tend to be higher. Inland, where lower wind speeds prevail, the GPBT is typically higher (up to 22.5 months). The average GPBT for wind turbines in northwestern Europe is 5.25 months.

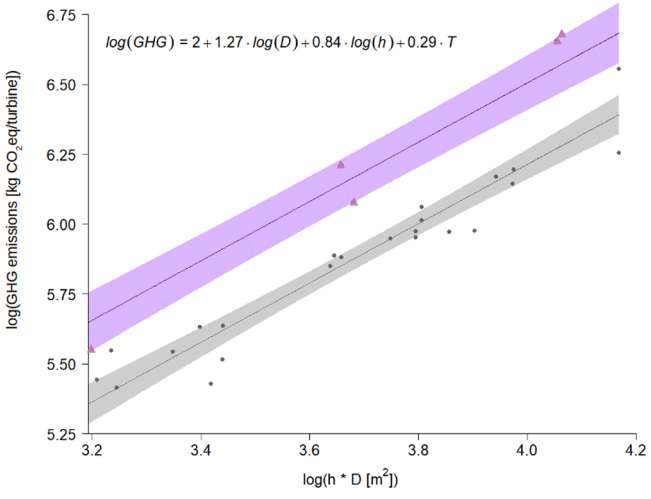

Figure 3. GHG emissions of onshore turbines (T = 0, gray line shading) and offshore turbines (T = 1, purple line shading) as a function of log(D·h). The shading represents the 95% confidence interval. The markers are the harmonized LCA results from the literature (circles are onshore and triangles offshore wind turbines).

Ignoring Variability in Wind Speed and Turbine Size. Spatially averaging wind speed while maintaining the hourly temporal resolution and the variation in turbine technology results in a poor match with the reference data (KGE = −0.27) (Figure 5a). This is due to a 2-fold underestimation of the GPBT (β = 1.93), while the spread in the GPBT is smaller than in the reference situation (γ = 0.27). The correlation between GPBTs of the spatially averaged wind speed and the reference situation is also relatively low (r = 0.53).

Using a time-averaged wind speed at a 2.5 by 2.5 km spatial resolution results in an even poorer match with the reference data with a KGE of −0.53 (Figure 5b). This low KGE value is mainly due to a large overestimation of the spread in GPBT (γ = 2.51). Averaging wind speed both spatially and temporally also gives a negative KGE of −0.26 (Figure 5c). Similar to the spatially homogeneous wind field, the average GPBT is strongly overestimated (β = 1.94).

Using an average turbine size for on- and offshore wind turbines results in a much higher KGE of 0.82 (Figure 5d), compared to neglecting climatological variability. The correlation coefficient is relatively high (r = 0.88), and systematic deviations of the mean and spread are relatively small (β = 1.12; γ = 1.06).

Spatial and Temporal Resolution. Figure 6 summarizes the influence of the spatial and temporal resolution on the KGE performance metric and its components. Figure 6a shows that decreasing the spatial resolution is the dominant factor for lowering the KGE, while temporal resolution (hourly vs daily wind speed estimations) has only a limited influence on the KGE. The lowest KGE is found for the spatial resolution of 80 by 80 km (KGE = 0.18−0.43). The 30 by 30 km resolution provides intermediate KGEs (0.65−0.75), while a 10 by 10 km resolution or higher always results in a KGE greater than 0.89. The relatively low KGE for the 80 by 80 km resolution is caused by an overestimation of the spread in GPBT (γ = 1.48−1.75; Figure 6c) in combination with a decrease in the correlation coefficient (r = 0.79−0.81; Figure 6d). The γ coefficient shows two interesting trends: it decreases with a decrease in temporal resolution, and it increases with a decrease in spatial resolution. These two trends counteract one another resulting in a higher KGE for the 80 by 80 km resolution with the lowest temporal resolution (24 hly).

DISCUSSION

Interpretation. The analysis showed that the spatial and temporal wind information are of particular importance when assessing the wind turbine greenhouse gas payback time, a fact that is often neglected in LCAs, while the variation in turbine size appears to be of relatively lower importance. The analysis further indicated that daily wind speed data on a 30 by 30 km grid provide results that still match the reference high-resolution data (KGE = 0.75), although a spatial resolution of 10 by 10 km would further improve model performance (KGE = 0.89).

When time-averaged wind speeds over 35 years were used as an extreme scenario, GPBTs were severely overestimated. Wind speed shows a non-normal temporal frequency

DOI: 10.1021/acs.est.9b01030
Environ. Sci. Technol. 2019, 53, 9289−9297

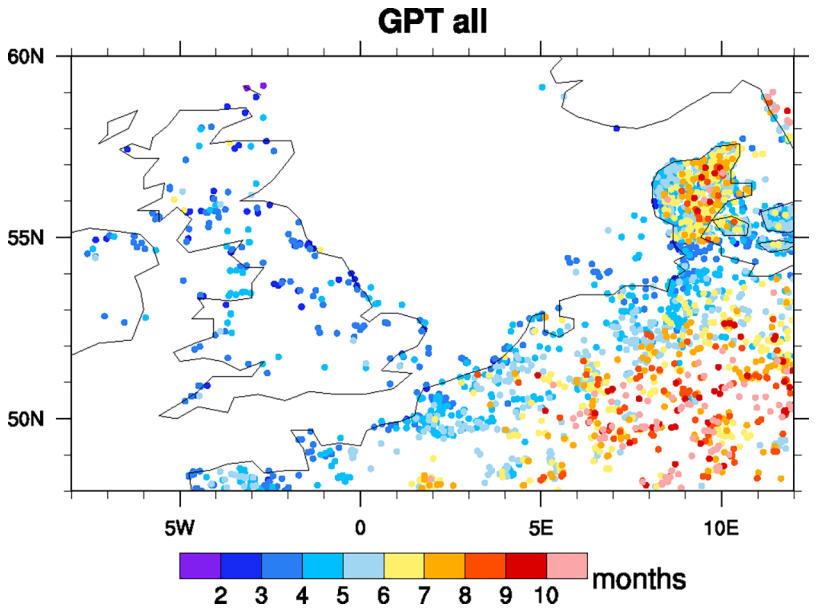

Figure 4. Greenhouse gas payback time (in months) for the reference situation (wind data at 2.5 by 2.5 km and hourly resolution and turbine-specific size characteristics).[46]

distribution, with lower wind speeds occurring more frequently than higher values.[35] Combined with the nonlinear dependence of the power output on the wind speed, the long-term average wind speed causes a strong underestimation of the power output and hence an overestimation of the GPBT. Using one daily wind speed value measured at noon performed equally well compared to the use of hourly data. In Europe, the average wind speed at noon is slightly higher than the daily mean for vertical levels up to 80 m.[47] Because more than 75% of the wind turbines included here have hub heights lower than 80 m, this leads to slightly higher power yields and consequently a 10% underestimation of GPBT compared to using the daily averaged wind data.

Completely neglecting spatial variability in the wind speed led to large over- and underestimations of GPBT of individual wind turbines. Although offshore wind turbines require more building materials (and hence have higher GHG emissions) than onshore installations, offshore GPBT are typically lower because of the higher wind speeds over sea. The results reflect, however, only a relatively small sample of only 80 offshore wind turbine locations; more offshore locations should be included to consolidate this conclusion.

Uncertainties. This study showed that it is highly relevant to account for spatiotemporal and technological variation when calculating the GPBT of wind electricity. A number of uncertainties may, however, influence the results, which are further discussed below.

First, wind farms were treated as a single geographical location, while in reality wind farms may occupy large surface areas. The largest farm in the data set (175 turbines with a diameter of 107 m) covers an area of approximately 56 km^2, thus covering multiple grid cells in the KNW-Atlas, which could each have a distinct wind climatology. However, less than 2% of the wind turbine locations in the data set span more than one grid cell and less than 0.6% more than two grid cells. Additionally, large wind farms are predominantly located offshore, where wind climatology is more stable because of low surface roughness.[35] Therefore, the effect of ignoring the spatial extent of wind farms is considered limited in the context of this study.

The power performance of wind turbines can also be influenced by wake effects. In a wind farm, downstream turbines are affected by a decrease in wind speed due to momentum loss caused by upstream turbines.[48] Several studies[35,49] report that power output in wind farms are typically 5 to 10% lower because of these wake effects, but losses could be as high as 50% in large farms with narrow turbine spacing.[50] Here, more than 75% of the locations consisted of fewer than 4 turbines and only 0.1% of the locations had array sizes exceeding 10 × 10 turbines. Wake effects therefore are unlikely to influence the GPBT calculations. Still, wake effects may become important for other locations in the world and as more large wind farms are built in the future.

Another source of uncertainty is that a resolution of 2.5 km is most likely not sufficient to capture the local properties of wind speed at the top of mountain ranges. The energy yield of a wind turbine at mountain tops is therefore most likely underestimated in this analysis. However, with increasing height the air density decreases, which also influences power performance. A recent study by Jung and Schindler[51] showed that at a height of 800 m, the highest elevation with wind turbines in the study area, annual energy yields are overestimated by 6% when changes in air density are not considered. The same error in GPBTs is achieved when taking one daily wind speed measure instead of hourly data or changing from a 2.5 by 2.5 km to a 5 by 5km grid. While the uncertainty from this simplification is not negligible, the 6% error in GPBT from neglecting air density changes is relatively small compared to the error introduced by using average wind speeds, as shown in the analysis. In areas with even higher elevations, spatiotemporal variance in air density should be accounted for because errors in energy yield can otherwise amount to up to 25%.

Incorporating more turbine-specific losses can further improve the GPBT calculations. Examples are performance decline due to aging, which has been reported to lie around

DOI: 10.1021/acs.est.9b01030
Environ. Sci. Technol. 2019, 53, 9289−9297

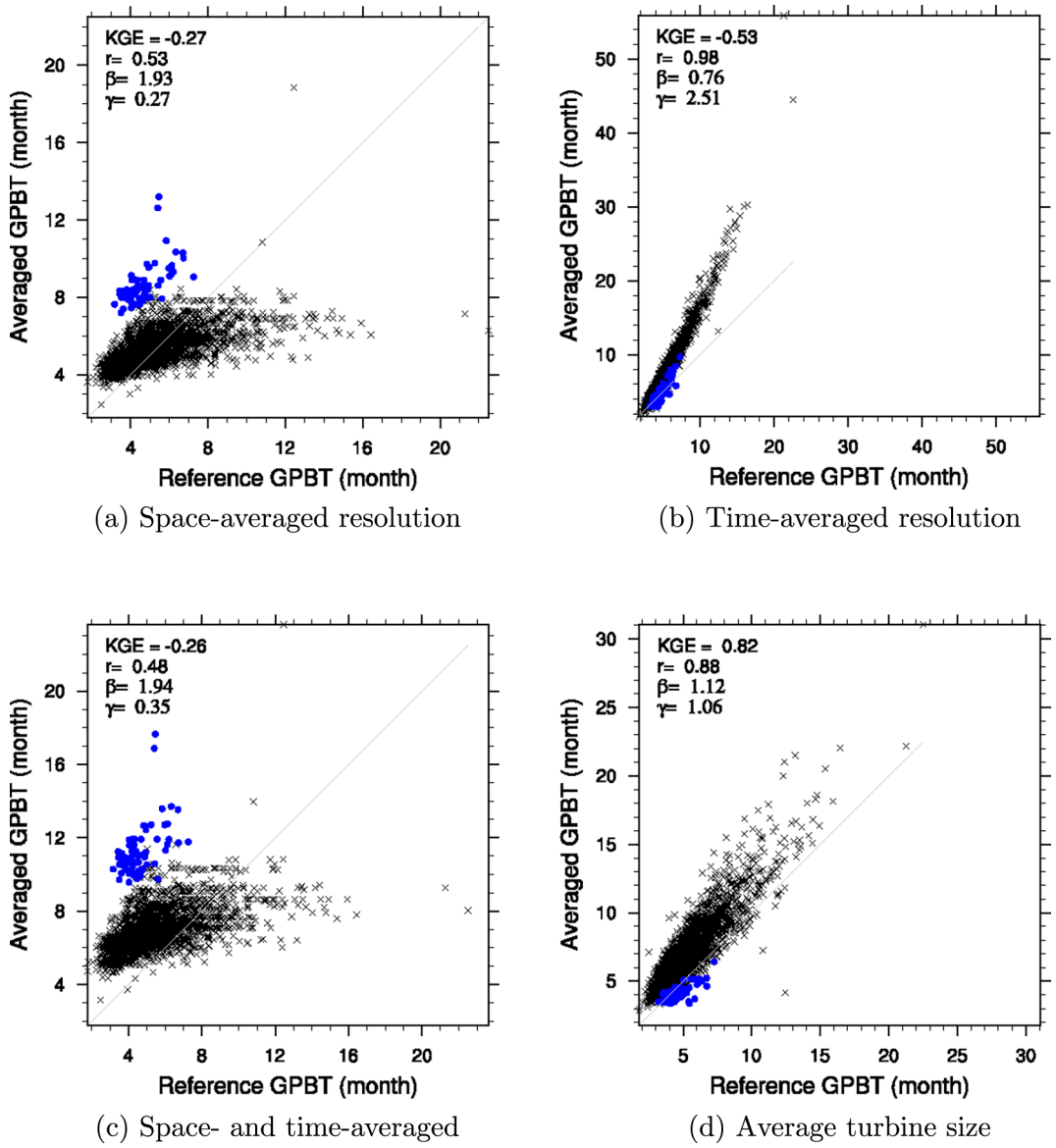

Figure 5. Comparison of greenhouse gas payback times (GPBT) for the reference scenario vs the scenarios with spatially averaged wind speed (a), time-averaged wind speed (b), wind speed averaged over space and time (c), and average turbine size for onshore and offshore farms (d). Offshore wind locations are represented by the blue dots, and onshore wind locations are represented by the black crosses. KGE is the Kling−Gupta efficiency, r the Pearson correlation coefficient, γ the variability ratio, and β the bias ratio.[46]

0.6% per year,[52] and losses due to rotor blade soiling and/or icing, which are generally assumed to account for 2%, but can in rare cases exceed 20%.[53]

Finally, a gas-fired power plant was chosen as the background energy system to focus the investigation on the effect of changes in wind climatology and turbine technology. More advanced reference systems that more precisely reflect what is replaced by the produced wind electricity can also be considered, but that would require a substantial amount of extra information about the electricity system as a whole.[54] Another possibility to evaluate the environmental trade offs of wind electricity is to integrate the location-specific long-term power output and material requirements for wind turbines into integrated assessment models.[55]

Outlook. The method presented here can be used to derive the environmental performance of current and future individual wind turbines worldwide even when limited information on turbine technology is available. Following the developments in the wind energy market to build larger wind farms, wake effects should be included in the future, and when areas with higher elevation are considered, the spatiotemporal variability in air density has to be considered.

Recent studies specifically focused on the energy production potential of wind turbines but did not consider environmental impacts such as GPBT[43,56,57] or use wind climatology that is either not globally available or at coarser resolutions. This study indicates that the use of current spatial resolution for global climate data archives (e.g., ERA-Interim[37]) of 80 by 80 km introduces a relatively large uncertainty in the power predictions (KGE = 0.18−0.43). A new ERA-suite, ERA5,[58] is under development with global climatological data at an hourly and 30 by 30 km resolution at which the KGE exceeds 0.7.

Therefore, using this method with the new ERA-suite would provide a good opportunity for location-specific predictions of the environmental impacts for wind turbines at the global scale. The method may also be used to identify optimal locations for

DOI: 10.1021/acs.est.9b01030
Environ. Sci. Technol. 2019, 53, 9289−9297

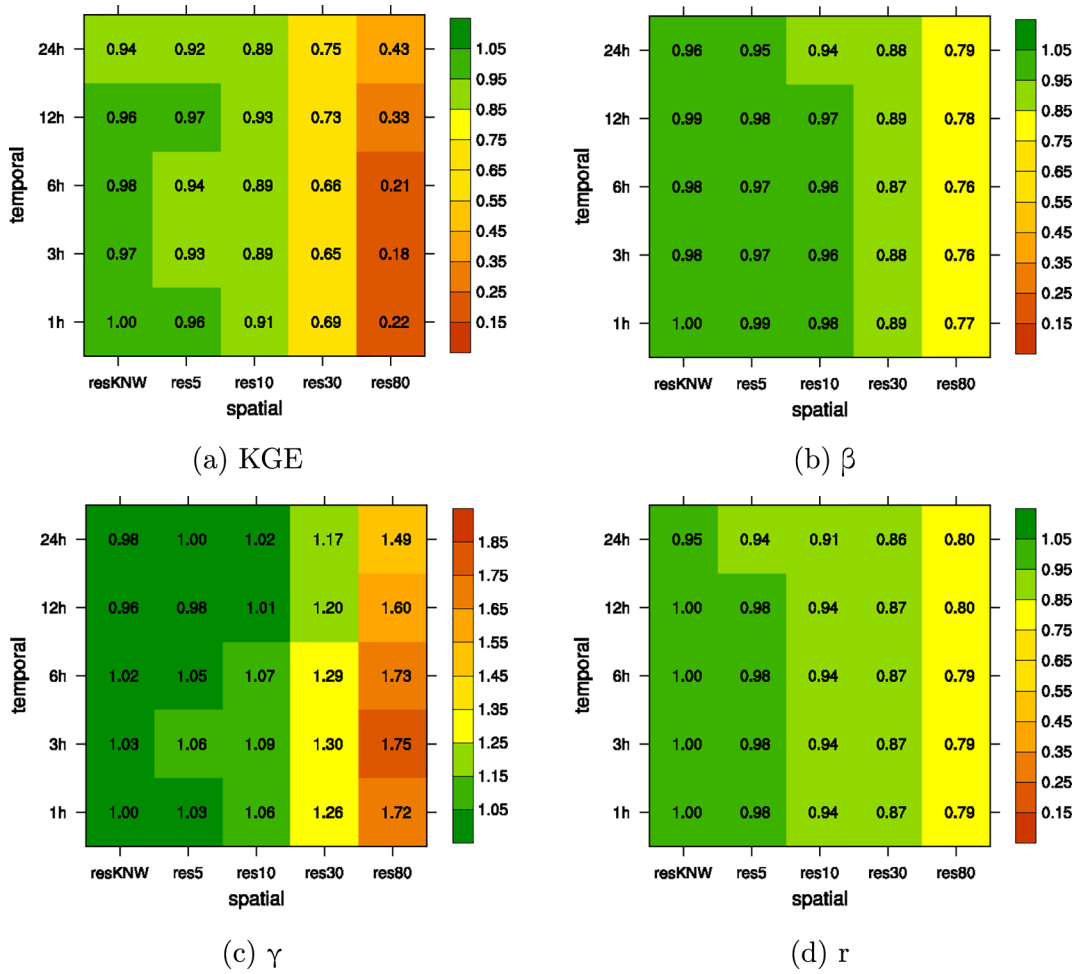

Figure 6. Kling–Gupta efficiency (a), Pearson correlation coefficient (b), variability ratio (c), and bias ratio (d) of the GPBT at various coarser spatial (5 by 5, 10 by 10, 30 by 30, and 80 by 80 km) and temporal resolutions (3, 6, 12, 24 hly) relative to the most detailed reference resolution (resKNW: hourly and 2.5 by 2.5 km).[46]

wind turbines taking into account environmental impacts. The results could be incorporated as an extra factor in wind energy potential studies for various regions worldwide. In addition to the GPBT, this method can also be used to calculate payback times for other environmental impacts, such as water and mineral resource scarcity,[59,60] giving a more complete picture of wind turbines' environmental performances.

This study showed that the GPBT of wind turbines in northwestern Europe varies between 1.8 and 22.5 months. Detailed spatiotemporal (at least daily wind speed on a 30 by 30 km grid) wind climatology as well as hub height and rotor diameter of the wind turbines are required to assess the greenhouse gas payback times of wind electricity with sufficient accuracy. The findings imply that a location-specific assessment of wind turbines' GPBTs at the global scale is well within reach with the availability of high-resolution reanalysis data sets and wind turbine databases.

AUTHOR INFORMATION

Corresponding Author

*E-mail: l.dammeier@science.ru.nl.

ORCID

Louise C. Dammeier: 0000-0002-5597-1811

Zoran J. N. Steinmann: 0000-0001-8606-917X

Notes

The authors declare no competing financial interest.

ACKNOWLEDGMENTS

This work is part of project number 016.Vici.170.190, which is financed by The Netherlands Organisation for Scientific Research (NWO). The TOC art graphic was created in part using matplotlib, hosted at https://github.com/matplotlib/matplotlib.

REFERENCES

(1) International Energy Agency. *Next Generation Wind and Solar Power - From cost to value*; Paris, FR, 2016.

(2) World Wind Energy Association. Wind Power Capacity Reaches 600 GW, 53,9 GW Added in 2018 [Online]; https://wwindea.org/blog/2019/02/25/wind-power-capacity-worldwide-reaches-600-gw-539-gw-added-in-2018/ (accessed April 10, 2019).

(3) International Energy Agency. *World Energy Outlook 2015*; Paris, FR, 2015.

(4) Global Wind Energy Council. *Global Wind Energy Outlook 2016*; Brussels, BE, 2016.

(5) Dolan, S. L.; Heath, G. A. Life cycle greenhouse gas emissions of utility-scale wind power. *J. Ind. Ecol.* **2012**, *16* (s1), S136–S154.

(6) International Organization for Standardization Home page. ISO 14040:2016; https://www.iso.org/standard/37456.html (accessed April 10, 2019).

DOI: 10.1021/acs.est.9b01030
Environ. Sci. Technol. 2019, 53, 9289–9297

(7) Bonou, A.; Laurent, A.; Olsen, S. I. Life cycle assessment of onshore and offshore wind energy - from theory to application. *Appl. Energy* **2016**, *180*, 327−337.
(8) Caduff, M.; Huijbregts, M. A. J.; Althaus, H.-J.; Koehler, A.; Hellweg, S. Wind Power Electricity: The Bigger the Turbine, The Greener the Electricity? *Environ. Sci. Technol.* **2012**, *46* (9), 4725−4733.
(9) Chen, G. Q.; Yang, Q.; Zhao, Y. H. Renewability of wind power in China: A case study of nonrenewable energy cost and greenhouse gas emission by a plant in Guangxi. *Renewable Sustainable Energy Rev.* **2011**, *15* (5), 2322−2329.
(10) Guezuraga, B.; Zauner, R.; Pölz, W. Life cycle assessment of two different 2 MW class wind turbines. *Renewable Energy* **2012**, *37* (1), 37−44.
(11) White, S.; Kulcinski, G. *Net energy payback and CO_2 emissions from wind-generated electricity in the Midwest*; UWFDM-1092 Fusion Technology Institute, Department of Engineering Physics, University of Wisconsin-Madison: Madison, WI, December 1998.
(12) White, S. W. Net energy payback and CO_2 emissions from three midwestern wind farms: an update. *Nat. Resour. Res.* **2007**, *15* (4), 271−281.
(13) Demir, N.; Taşkin, A. Life cycle assessment of wind turbines in Pınarbaşı-Kayseri. *J. Cleaner Prod.* **2013**, *54*, 253−263.
(14) Padey, P.; Girard, R.; le Boulch, D.; Blanc, I. From LCAs to Simplified Models: A Generic Methodology Applied to Wind Power Electricity. *Environ. Sci. Technol.* **2013**, *47* (3), 1231−1238.
(15) Sacchi, R.; Besseau, R.; Pérez-López, P.; Blanc, I. Exploring technologically and geographically-sensitive life cycle inventories for wind turbines: A parameterized model for Denmark. *Renewable Energy* **2019**, *132*, 1238−1250.
(16) Besseau, R.; Sacchi, R.; Blanc, I.; Pérez-López, P. Past, present and future environmental footprint of the Danish wind turbine fleet with LCA_WIND_DK, an online interactive platform. *Renewable Sustainable Energy Rev.* **2019**, *108*, 274−288.
(17) Elshout, P. M. F.; van Zelm, R.; Balkovic, J.; Obersteiner, M.; Schmid, E.; Skalsky, R.; van der Velde, M.; Huijbregts, M. A. J. Greenhouse-gas payback times for crop-based biofuels. *Nat. Clim. Change* **2015**, *5*, 604−610.
(18) Royal Netherlands Meteorological Institute Home Page. KNW (KNMI North sea Wind) Atlas. http://projects.knmi.nl/knw/ (accessed April 10, 2019).
(19) The Wind Power. Wind farms databases. http://www.thewindpower.net/index.php (accessed August 21, 2018).
(20) Hertwich, E. G.; Gibon, T.; Bouman, E. A.; Arvesen, A.; Suh, S.; Heath, G. A.; Bergesen, J. D.; Ramirez, A.; Vega, M. I.; Shi, L. Integrated life-cycle assessment of electricity-supply scenarios confirms global environmental benefit of low-carbon technologies. *Proc. Natl. Acad. Sci. U. S. A.* **2015**, *112* (20), 6277−6282.
(21) Nalukowe, B. B.; Liu, J.; Damien, W.; Lukawski, T. *Life cycle assessment of a wind turbine*. Report 1N1800 2006.
(22) Vestas Wind Systems A/S. *Life Cycle Assessment of Electricity Productiom from a V80-2.0 MW Gridstreamer Wind Plant*; Randers, DK, 2011; https://www.vestas.com/~/media/vestas/about/sustainability/pdfs/lca_v802mw_version1.pdf.
(23) Elsam Engineering A/S. *Life Cycle Assessment of offshore and onshore sited wind farms (Engl. Transl.)*; Copenhagen, DK, 2004; https://www.vestas.com/~/media/vestas/about/sustainability/pdfs/lca_v80_2004_uk.ashx.
(24) Vestas Wind Systems A/S. *Life Cycle Assessment of Electricity Production from an onshore V126-3.3 MW Wind Plant*; Randers, DK, 2014; https://www.vestas.com/~/media/vestas/about/sustainability/pdfs/lcav12633mwfinal060614.pdf.
(25) Vestas Wind Systems A/S. *Life Cycle Assessment of Electricity Production from an onshore V100-2.0 MW Wind Plant*; Randers, Denmark, 2015; https://www.vestas.com/~/media/vestas/about/sustainability/pdfs/lcav10020mw181215.pdf.
(26) Haapala, K. R.; Prempreeda, P. Comparative life cycle assessment of 2.0 MW wind turbines. *Int. J. Sustainable Manuf.* **2014**, *3* (2), 170−185.
(27) ecoinvent Centre. *Life cycle inventories of energy systems: Results for current systems in Switzerland and other UCTE countries*; Dübendorf, CH, 2007; ecolo.org/documents/documents_in_english/Life-cycle-analysis-PSI-05.pdf.
(28) Rashedi, A.; Sridhar, I.; Tseng, K. Life cycle assessment of 50MW wind firms and strategies for impact reduction. *Renewable Sustainable Energy Rev.* **2013**, *21*, 89−101.
(29) Bundesamt für Energie BFE. *Ökobilanzierung von Schweizer Windenergie*; Bern, CH, 2015; https://www.zhaw.ch/storage/lsfm/institute-zentren/iunr/oekobilanzierung/eymann-2015-lca-windenergie-bfe.pdf.
(30) Pick, E.; Wagner, H.-J.; Bunk, O. Kumulierter Energieaufwand von Windkraftanlagen. *Brennstoff-Wärme-Kraft* **1998**, *50*, 52−55.
(31) Vestas Wind Systems A/S. *Life Cycle Assessment of Electricity Production from a V90-2.0 MW Gridstreamer Wind Plant*. Randers, DK, 2011; https://www.vestas.com/~/media/vestas/about/sustainability/pdfs/lca_v902mw_version1.pdf.
(32) Vestas Wind Systems A/S. *Life Cycle Assessment of Electricity Production from a V112 Turbine Wind Plant*. Randers, DK, 2011; https://www.vestas.com/~/media/vestas/about/sustainability/pdfs/lca_v112_study_report_2011.pdf.
(33) Arvesen, A.; Hertwich, E. G. Assessing the life cycle environmental impacts of wind power: A review of present knowledge and research needs. *Renewable Sustainable Energy Rev.* **2012**, *16* (8), 5994−6006.
(34) Arlot, S.; Celisse, A. A survey of cross-validation procedures for model selection. *Stat. Surv.* **2010**, *4*, 40−79.
(35) European Wind Energy Association. *The Economics of Wind Energy - A report by the European Wind Energy Association*; Brussels, BE, 2009.
(36) Betz, A. *Introduction to the Theory of Flow Machines*; Pergamon Press: Oxford, U.K., 1966.
(37) Dee, D. P.; Uppala, S. M.; Simmons, A. J.; Berrisford, P.; Poli, P.; Kobayashi, S.; Andrea, U.; Balmaseda, M. A.; Balsami, G.; Bauer, P.; Bechtold, P.; Beljaars, A. C. M.; van den Berg, L.; Bidlot, J.; Bormann, N.; Delsol, C.; Dragani, R.; Fuentes, M.; Geer, A. J.; Haimberger, L.; Healy, S. B.; Hersbach, H.; Hólm, E. V.; Isaksen, L.; Kållberg, P.; Köhler, M.; Matricardi, M.; McNally, A. P.; Monge-Sanz, B. M.; Morcrette, J.-J.; Park, B.-K.; Peubey, C.; de Rosnay, P.; Tavolato, C.; Thépaut, J.-N.; Vitart, F. The ERA-Interim reanalysis: configuration and performance of the data assimilation system. *Q. J. R. Meteorol. Soc.* **2011**, *137* (656), 553−597.
(38) Bubnová, R.; Hello, G.; Bénard, P.; Geleyn, J.-F. Integration of the fully elastic equations cast in the hydrostatic pressure terrain-following coordinate in the framework of the arpege/aladin nwp system. *Mon. Weather Rev.* **1995**, *123*, 515−535.
(39) Seity, Y.; Brousseau, P.; Malardel, S.; Hello, G.; Bénard, P.; Bouttier, F.; Lac, C.; Masson, V. The AROME-France Convective-Scale Operational Model. *Mon. Weather Rev.* **2011**, *139*, 976−991.
(40) Stepek, A.; Savenije, M.; van den Brink, H. W.; Wijnant, I. L. *Validation of KNW atlas with publicly available mast observations (Phase 3 of KNW project)*; Technical Report TR-352 for the Royal Netherlands Meteorological Institut: De Bilt, NL, April 2015.
(41) Weijnant, I. L.; Marseille, G. J.; van den Brink, H. W.; Stepke, A. *Validation of the KNW Atlas with scatterometer winds (Phase 3 of KNW project)*; Technical Report TR-353 for the Royal Netherlands Meteorological Institute: De Bilt, NL, April 2015.
(42) Kling, H.; Fuchs, M.; Paulin, M. Runoff conditions in the upper Danube basin under an ensemble of climate change scenarios. *J. Hydrol.* **2012**, *424*−*425*, 264−277.
(43) González-Aparicio, I.; Monforti, F.; Volker, P.; Zucker, A.; Careri, F.; Huld, T.; Badger, J. Simulating European wind power generation applying statistical downscaling to reanalysis data. *Appl. Energy* **2017**, *199*, 155−168.
(44) Dee, D.; Fasullo, J.; Shea, D.; Walsh, J., NCAR Staff. The Climate Data Guide: Atmospheric Reanalysis: Overview & Comparison Tables. https://climatedataguide.ucar.edu/climate-data/atmospheric-reanalysis-overview-comparison-tables (accessed April 10, 2019).

DOI: 10.1021/acs.est.9b01030
Environ. Sci. Technol. 2019, 53, 9289−9297

(45) Flato, G.; Marotzke, J.; Abiodun, B.; Braconnot, P.; Chou, S. C.; Collins, W.; Cox, P.; Driouech, F.; Emori, S.; Eyring, V.; Forest, C.; Gleckler, P.; Guilyardi, E.; Jakob, C.; Kattsov, V.; Reason, C.; Rummukainen, M. Evaluation of Climate Models. In *Climate Change 2013: The Physical Science Basis. Contribution of Working Group I to the Fifth Assessment Report of the IPCC*; Stocker, T. F., Qin, D., Plattner, G.-K., Tignor, M., Allen, S. K., Boschgun, J., Nauels, A., Xia, Y., Bex, V., Midgley, P. M., Eds.; Cambridge University Press: Cambridge, U.K., 2013.
(46) *The NCAR Command Language*, version 6.4.0; Boulder, Colorado, 2017.
(47) Fajber, R.; Monahan, A. H.; Merryfield, W. J. At What Time of Day Do Daily Extreme Near-Surface Wind Speeds Occur? *J. Clim.* **2014**, *27*, 4226−4244.
(48) Son, E.; Lee, S.; Hwang, B.; Lee, S. Characteristics of turbine spacing in a wind farm using optimal design process. *Renewable Energy* **2014**, *65*, 245−249.
(49) Barthelmie, R. J.; Pryor, S. C.; Frandsen, S. T.; Hansen, K. S.; Schepers, J. G.; Rados, K.; Schlez, W.; Neubert, A.; Jensen, L. E.; Neckelmann, S. Quantifying the Impact of Wind Turbine Wakes on Power Output at Offshore Wind Farms. *J. Atmos. Oceanic Technol.* **2010**, *27*, 1302−1317.
(50) Dupont, E.; Koppelaar, R.; Jeanmart, H. Global available wind energy with physical and energy constraints. *Appl. Energy* **2018**, *209*, 322−338.
(51) Jung, C.; Schindler, D. The role of air density in wind energy assessment - A case study from Germany. *Energy* **2019**, *171*, 385−392.
(52) Germer, S.; Kleidon, A. Have wind turbines in Germany generated electricity as would be expected from the prevailing wind conditions in 2000−2014? *PLoS One* **2019**, *14* (2), e0211028.
(53) Dalili, N.; Edrisy, A.; Carriveau, R. A review of engineering issues critical to wind turbine performance. *Renewable Sustainable Energy Rev.* **2009**, *13* (2), 428−438.
(54) Siler-Evans, K.; Azevedo, I. L.; Morgan, M. G.; Apt, J. Regional variations in the health, environmental, and climate benefits of wind and solar generation. *Proc. Natl. Acad. Sci. U. S. A.* **2013**, *110* (29), 11768−11773.
(55) Pehl, M.; Arvesen, A.; Humpenöder, F.; Popp, A.; Hertwich, E. G.; Luderer, G. Understanding future emissions from low-carbon power systems by integration of life-cycle assessment and integrated energy modelling. *Nat. Energy* **2017**, *2*, 939−945.
(56) Dabbaghiyan, A.; Fazelpour, F.; Mohhamadreza, D. A.; Rosen, M. A. Evaluation of wind energy potential in province of Bushehr, Iran. *Renewable Sustainable Energy Rev.* **2016**, *55*, 455−466.
(57) Allouhi, A.; Zamzoum, O.; Islam, M. R.; Saidur, R.; Kousksou, T.; Jamil, A.; Derouich, A. Evaluation of wind energy potential in Morocco's coastal regions. *Renewable Sustainable Energy Rev.* **2017**, *72*, 311−324.
(58) ECMWF. ERA5. https://www.ecmwf.int/en/forecasts/datasets/reanalysis-datasets/era5 (accessed April 10, 2019).
(59) Vieira, M. D. M.; Ponsioen, T. C.; Goedkoop, M. J.; Huijbregts, M. A. J. Surplus Ore Potential as a Scarcity Indicator for Resource Extraction. *J. Ind. Ecol.* **2017**, *21* (2), 381−390.
(60) Pfister, S.; Saner, D.; Koehler, A. The environmental relevance of freshwater consumption in global power production. *Int. J. Life Cycle Assess.* **2011**, *16* (6), 580−591.

DOI: 10.1021/acs.est.9b01030
Environ. Sci. Technol. 2019, 53, 9289−9297